Creation of Digital Terrain Models Using an Adaptive Lidar Vegetation Point Removal Process

George T. Raber, John R. Jensen, Steven R. Schill, and Karen Schuckman

Abstract

Commercial small-footprint lidar remote sensing has become an established tool for the creation of digital terrain models (DTMs). Unfortunately, even after the application of lidar vegetation point removal algorithms, vertical DTM error is not uniform and varies according to land cover. This paper presents the results of the application of an adaptive lidar vegetation removal process to a raw lidar dataset of a small area in North Carolina. This process utilized an existing lidar vegetation point removal algorithm in which the parameters were adaptively adjusted based on a vegetation map. The vegetation map was derived through the exclusive use of the lidar dataset, making the process independent of ancillary data. The vertical error and surface form of the resulting DTM were then compared to DTMs created using traditional techniques. The results indicate that the adaptive method produces a superior DTM.

Introduction

Digital terrain models (DTMs) are used to model landscape elevation, slope, and aspect characteristics for hydrologic, environmental, and urban/suburban applications. Methods for creating DTMs include (1) *in situ* measurement using surveying instruments (including the Global Positioning System), (2) photogrammetric techniques based on stereoscopic aerial photography, (3) interferometric synthetic aperture radar (IFSAR), and (4) active light detection and ranging (lidar) technology (Jensen, 2000). Each method has strengths and weaknesses and produces DTMs of varying accuracy. Recently, there has been confusion in the DTM marketplace regarding which method is superior. As a response to this, there has been a significant amount of research conducted to determine the best methods for creating accurate bald-earth surface DTMs using lidar technology (e.g., Plaut *et al.*, 1999; Hodgson *et al.*, 2002). This research describes adaptive digital image post-processing techniques that can be used to create more accurate DTMs using lidar-derived vegetation canopy information.

Multiple-Return Lidar Characteristics

The majority of current lidar instruments receive multiple returns from a single transmitted laser pulse. This is commonly referred to as "multiple-return" lidar. The interaction of the laser pulse with the Earth's surface may be relatively simple or complex. In the simplest case, a pulse of laser energy interacts directly with bare soil, asphalt, and/or concrete, and most of it is scattered back toward the receiver. This results in a single return. Similarly, depending upon the wavelength of the laser, a single laser pulse may be scattered directly from the top of a very dense vegetation canopy, also resulting in a single return (although this is less likely). The situation becomes more complex when a pulse of laser energy passes through the top of the canopy and interacts with (1) the tree canopy trunk, branches, stems, and leaves; (2) understory trunk, branches, stems, and leaves; and, finally, (3) the terrain surface. This series of events may result in several returns being recorded for a single pulse of transmitted energy. Current commercial lidar instruments generate, at this writing, 5,000 to 50,000 pulses per second, each of which may produce several returns. A detailed discussion of lidar technology, capabilities, and application is available in Maune (2001).

Improving the Accuracy of Lidar-Derived DTMs

It is necessary to identify and segregate lidar returns that hit the terrain surface from non-terrain surface returns (e.g., within the vegetation canopy) in order to create accurate lidar-derived DTMs. To this end, research has been conducted to assess the accuracy and the potential sources of error in DTMs. For example, Huising *et al.* (1998) examined the impact of instrument and calibration error on lidar-derived DTMs. Cowen *et al.* (2000) evaluated the effect of percent canopy closure on lidar-derived DTMs. Hodgson *et al.* (2003) found that land-cover types were a significant factor when extracting elevation information from leaf-on lidar data in North Carolina.

Setting aside instrument error (i.e., assuming all recorded lidar observation points are in their precise planimetric location), there are theoretically two major explanations for the introduction of lidar-produced DTM error: (1) interpolation error, and (2) error that results from the incorporation of non-terrain points in the creation of the DTM. Interpolation error has two major sources. The first source of interpolation error is semi-systematic because it is related to the post spacing or distance between lidar returns (e.g., 3 meters between lidar return postings). Post spacing is the result of a number of collection parameters, including (1) flying height of the aircraft above ground level (AGL), (2) speed of the aircraft, (3) the pulse rate, and (4) the scan angle.

The second source of interpolation error is a result of the lidar vegetation point removal process. Many common lidar vegetation point removal algorithms use a statistical surface trend to remove lidar-derived elevation points that appear to be the result of interaction with vegetation cover rather than the desired bald earth (Tao and Hu, 2001; Kraus and Pfeifer, 1998). The removal of lidar vegetation points means that fewer points are available for interpolation in certain areas (i.e., data voids exist). In addition, if true bald-earth lidar points are mistakenly

G.T. Raber, J.R. Jensen, and S.R. Schill are with the Department of Geography, University of South Carolina, Columbia, SC 29208 (gr@sc.edu).

K. Schuckman is with EarthData Technologies, LLC, 1912 Eastchester Drive, High Point, NC 27265.

Photogrammetric Engineering & Remote Sensing
Vol. 68, No. 12, December 2002, pp. 1307–1315.

0099-1112/02/6812–1307$3.00/0

removed because they are confused with non-ground points, additional interpolation error may be introduced. Both conditions most often cause under-prediction of terrain elevation because high slopes are smoothed and small peaks are removed (Figure 1). This type of error often appears in patterns (not random) because it is the result of smoothing a slope, or clipping a peak. When non-ground lidar points are used in the interpolation process, processed terrain elevation will be overestimated in the DTM (Figure 1).

The goal in the DTM creation process is to have a lidar vegetation point removal algorithm that results in the least overall DTM error. To date, little research has been conducted to account for the different types of vegetation encountered during the lidar vegetation point removal process. This study compares vertical DTM accuracy in DTMs produced using traditional lidar vegetation point removal techniques to a DTM created using a more sophisticated *adaptive* lidar vegetation point removal technique. The adaptive technique minimizes the overall error by applying different vegetation point removal parameters based on information the lidar data itself reveals about the vegetation type (land-cover class) present.

Lidar-Derived Vegetation Information

A multiple-return lidar system records the three-dimensional location of large numbers of points beneath the aircraft. In vegetated or built-up areas many of these points are not on the terrain surface. Previous research has suggested that some of this information can be used to characterize vegetation for environmental and forestry applications. For example, a number of studies us large-footprint Scanning Lidar Imager of Canopies and Echo overy (SLICER) data to measure vegetation characteristic· SLICER instrument only recorded five samples, or footp , for each scan. Because one footprint is 10 meters acr· de swath width is approximately 50 meters (Lefsky, 19· ,). Means *et al.* (1999) correlated characteristics of the SLICER waveform with *in situ* canopy height measurements. Such large-footprint lidar data are not commercially available.

Only a few studies have used conventional, small-footprint lidar data to extract vegetation characteristics. Jensen *et al.* (1987) used first- and last-return lidar data to obtain bottomland hardwood wetland tree height information. Næsset (1996) used last-return lidar data to predict mean height within forest stands ($r^2 = 0.91$). Means *et al.* (2000) achieved good predictions ($r^2 > 0.90$) of height, volume, and basal area using lidar-derived indices created by using aggregate statistical values derived from lidar points found within each cell of a 10- by 10-m grid. Height was estimated using the 90th percentile of the range (max-min return) and the average maximum height of the first return. Volume and basal area were estimated based on the relative height positions of the vertical point distributions at various percentiles of those distributions. A number of studies conducted as part of the European Union HIGH-SCAN project have also explored the link between lidar data and vegetation characteristics. Hyppä and Hyppä (1999) tested the ability of a number of remote sensing instruments, including SPOT, TM, and LIDAR data, to predict forest stand attributes, including height and stem volume. They found that lidar data predicted these relationships better than did the other sensors. Hyppä and Inkinen (1999) demonstrated a technique that employs lidar data collected with a high measurement density (4 to 5 per m^2) to predict attributes for individual tree crowns.

Results from these studies suggest that useful vegetation information can be extracted from multiple-return, small-footprint lidar data. This paper evaluates a unique method that was developed to identify vegetation characteristics based on information derived *exclusively* from multiple-return lidar data. The resulting vegetation classification information derived from the lidar data were then input to an *adaptive* lidar vegetation point removal algorithm to determine if it increased the accuracy of the resultant bald-earth DTM.

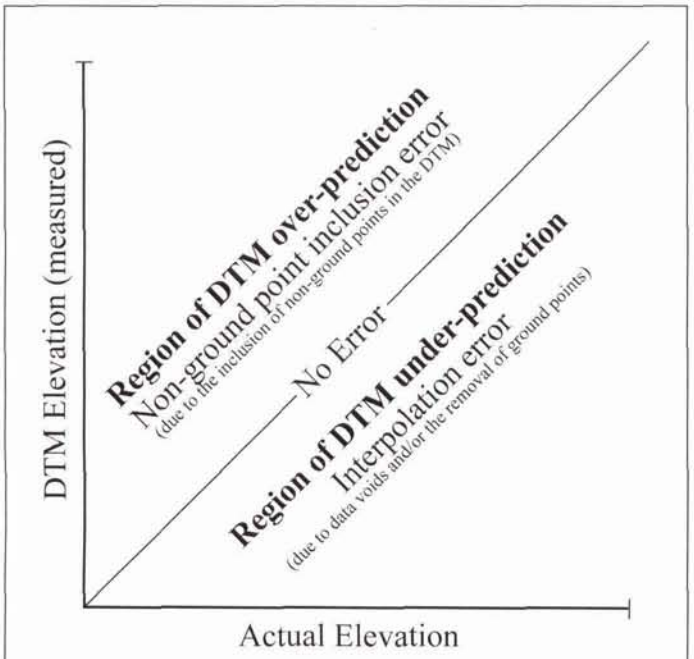

Figure 1. A model of the vertical error present in a lidar-derived DTM after the vegetation point removal process has been preformed. This model assumes no instrument error (i.e., assuming all recorded lidar observation points are in their precise planimetric location.)

Study Area

Hurricane Floyd made landfall in North Carolina on 16 September 1999. The storm remained over North Carolina for several days, causing an estimated $3.5 billion in damage, mostly from flooding. This catastrophic event revealed that current flood plain maps need to be updated. Consequently, North Carolina agencies decided to re-map the entire state using lidar to obtain an accurate bald-earth DTM. The statewide DTM will be used to predict areas at risk during any future flood event. The lidar research in this paper was initiated as a partnership between the NASA Affiliated Research Center at the University of South Carolina, the North Carolina Geodetic Survey, and EarthData, International of North Carolina, LLC., one of the contactors for the North Carolina mapping project.

The 3.25- by 3.5-km study area was in eastern North Carolina approximately 42 km northwest of Rocky Mount and 70 km northeast of Raleigh (Figure 2). The area was in the coastal plain and consisted primarily of agriculture and forest with very few buildings (less than ten farmhouses and related structures). Agriculture consisted of tobacco, soybean, corn, cotton, and alfalfa. Forest cover consisted of deciduous, coniferous, and mixed stands. Many of the coniferous stands were plantation pine at various levels of maturity. Elevation in the study area ranged from 50 to 80 m above sea level. For the most part, the terrain was gently rolling with little dramatic variation. Red Bud Creek and Swift Creek converge near the center of the study area. Small valleys created by these two creeks add the important elements of terrain variation and dense riparian vegetation to the study area.

Methodology

This study investigated several of the basic theoretical problems associated with the traditional approach to removing

Figure 2. The location of the study site is shown as a square on this map of the counties of North Carolina.

lidar returns in vegetated canopies. These problems include (1) traditional methods usually require a large amount of costly human supervision and manual editing, (2) they are typically inconsistent in the application of parameters especially in large projects, and (3) the lidar vegetation point removal algorithms usually treat the entire dataset equally, i.e., they are not "adaptive" to local, site-specific conditions. It was hoped that these problems would be minimized by the use of an adaptive lidar vegetation point removal algorithm that incorporates vegetation type information. Three hypotheses were tested in relation to the following objectives:

- Information contained in the vertical distribution of lidar points can be used to classify vegetation cover type,
- Digital terrain model elevation accuracy can be improved through an adaptive application of a lidar vegetation point removal algorithm that incorporates lidar-derived vegetation type information, and
- Digital terrain model surface form (slope) can be improved through an adaptive application of a lidar vegetation point removal algorithm that incorporates lidar-derived vegetation type information.

These hypotheses, stated above in alternative form, were tested in two separate phases. The first phase involved the extraction of vegetation type information using only lidar data. The second phase compared DTM results from

(a) the application of a traditional, *automatic* lidar vegetation point removal algorithm consisting of a single set of algorithm parameters determined by a human operator,
(b) a *human-edited* version of the results from (a) above,
(c) an *optimized* version of the *automatic* lidar vegetation point removal algorithm in (a) consisting of a single set of algorithm parameters determined through an automatic optimization process, and
(d) an *adaptive* lidar vegetation point removal algorithm where different algorithm parameters were developed for each land-cover class. Land-cover classes derived from the lidar data; each set of parameters determined through the automatic optimization process in (c) above.

Lidar Data Collection

The lidar data were collected by EarthData, using the AeroScan lidar instrument on 12 June 2000, during *leaf-on* conditions. The instrument was flown at 5,000 ft (1524 m) AGL to obtain a 3-meter post spacing, i.e., the lidar points were on average 3 meters apart. The instrument transmitted 15,000 pulses per second and collected up to five returns from each pulse. The lidar data were processed by EarthData and delivered as *x,y,z* ASCII files. A total of three lidar datasets were provided by EarthData, including:

- *Raw Returns*: Lidar-derived elevation postings processed to remove known instrument error.
- *Automatic*: Lidar-derived elevation postings after the application of a traditional vegetation removal algorithm.
- *Automatic with Human Editing*: Automatically processed data subjected to human manual editing. This is the product EarthData normally delivers to a customer that has requested a bald-earth DTM.

The raw return lidar data were merged from three different flight lines into a single dataset that was clipped to the study area boundary. Obvious "blunder" elevation postings that were vertically well above the main point cloud were discarded automatically based on a threshold value. These postings were most likely the result of some airborne object (e.g., a bird). The lidar data were then converted to ESRI point Shapefiles.

Reference Data

Three different sets of reference data were collected to test the hypotheses: (1) high spatial resolution color-infrared aerial photography, (2) ground-surveyed elevation data, and (3) *in situ* vegetated land-cover class observations. Stereoscopic 1:20,000-scale color-infrared aerial photography was collected on 15 September 2000 (Figure 3). The photography was digitized and orthorectified to 0.5- by 0.5-m pixels, and was used in the reference, training, and error assessment phases of the project. The land cover in the study area was exceptionally stable over the two-month period between the collection of the lidar data and the aerial photography.

Approximately 650 surveyed ground elevation points were collected by personnel of the North Carolina Geodetic Survey (NCGS) and National Aeronautics and Space Administration (NASA) using survey grade GPS units with an accuracy of ≤ 1 cm in the horizontal (X, Y) and vertical (Z). The points were obtained at approximately 5- to 6-m intervals along six transects which ran across stream channels to capture information on terrain variation. The vegetation land cover was measured *in situ* at approximately 500 observations along the six transects. This information was used to assess the accuracy of the land-cover classification map derived strictly from the lidar data, and to calibrate the lidar vegetation point removal algorithms.

Vegetation Classification Using Only Lidar Data

One goal of this research was to derive vegetation type information using only lidar data. If successful, land-cover information could be used adaptively in a lidar vegetation point removal algorithm to produce more accurate DTMs. The land-cover classification system used to characterize the land cover in the study area is summarized in Table 1.

The methodology to extract vegetation class information from lidar data was initiated by first examining the vertical distribution of the lidar elevation points. Multiple-return lidar data collected in forested environments is often characterized

Figure 3. A black-and-white reproduction of a 1:20,000-scale color-infrared photograph of the study area.

by point distributions throughout the top of the canopy, the mid-canopy and understory vegetation, and finally the terrain surface (Figure 4a). Rendering these points graphically yields a lidar "point cloud" pattern that can be used to appreciate the vertical structure of the ground cover (Figure 4b). Integrating the point cloud over a 15- by 15-m geographic area yielded a histogram that revealed the frequency of laser returns along the *Z*-axis (Figure 4c). This histogram is similar to a waveform because it changes based on the vertical vegetation structure present within each 15- by 15-m geographic area. Blair and Hoften (1999) referred to a similar histogram as the vertical distribution of intercepted surfaces (VDIS). Interestingly, Blair and Hoften (1999) used only single-return lidar data. They applied a transformation to the VDIS that considered the *intensity* of the return to produce a "pseudo-waveform." Conversely, this study is different because the vertical histograms created for it were based on multiple-return lidar information. These histograms did not include lidar intensity information.

Extracting vegetation land-cover type information using only lidar multiple-return data is based on the assumption that the vertical histogram changes with the distribution of the points, which in turn changes based on the type of vegetation cover. For example, the monoculture canopy, depicted in Figure 4a, and the terrain surface are discernible as the two modes of the distribution in the vertical histogram (Figure 4c). When mixed canopies are encountered, however, the bi-modal histogram tends to be dampened when compared to monoculture forest stands (not shown). Very open canopies or fields will create a histogram with only one mode because most of the points occur at the terrain surface (not shown).

To characterize these distributions over small areas, software was written to analyze and display statistics generated from the lidar data in a raster format. The software calculated aggregate statistics based on the vertical distribution of points within a specified kernel and stored the values in an output grid of specified cell size. For example, if a kernel of 15 by 15 m and an output grid cell size of 3 by 3 m was chosen, a moving window would create a 3- by 3-m grid of the study area in which each of the output cells would carry the values of various statistics of the vertical distribution of points (relative *Z*-values) for a 15- by 15-m box surrounding the center of each 3- by 3-m cell. Because the lidar post spacing for the project dataset was 3 m, a 15- by 15-m kernel size was chosen because this size would provide for a minimum of 25 points falling within the kernel area. Initially, only four distribution descriptors were calculated, thus creating a four-band image. These descriptors were the mean, standard deviation, range, and skewness. This image was classified but yielded only moderately accurate results.

To improve upon the lidar-based vegetation classification methodology, the program was modified to create the entire vertical histogram. This modification produced a 20-band image wherein each band represented a histogram bin. In other words, the set of bands for each cell of the image was a histogram, similar to the one in Figure 4c, which characterized the distribution of the vegetation in the 15- by 15-m kernel that was defined by that particular cell. Each histogram bin was 2 meters wide. No vegetation existed at greater than 40 meters above the minimum *Z*-value contained in any particular kernel; therefore, there were 20 bands. The initial result of this process was interesting and visually revealed different land-cover types. However, there were two problems with this statistical image stemming from the fact that it had 20 different bands. The high number of bands required a high amount of training data. The standard for training pixels is to have no fewer than 10 times the amount of bands for each class. Another problem was that the histogram was noisy. Due to the narrow bin sizes, there were very few returns in many classes, so that by chance two nearly identical vegetation type distributions could appear quite different, especially if the number of observations was low.

In order to reduce the noise and number of bands, a sample of ten points contained in each kernel was selected. One point was sampled at each 10th percentile of height from the minimum value. The *Z*-value of each of these points above the minimum point (relative *Z*-value) became the value for ten bands contained within the new image. The mathematical explanation of the process is based on the following equation:

$$V_{ijk} = P_{k*10}\,(Z_{X_iY_j}) \quad (1)$$

where V_{ijk} is the value of the statistical image at row i, column j, and band k; X_i and Y_j represent the real world coordinates at

TABLE 1. LAND-COVER CLASSES AND DESCRIPTIONS USED IN THE CLASSIFICATION PROCESS

Class	Description
Pine	• Natural growth forested areas dominated by pine species
	• Plantation pine
Deciduous	• Forested areas dominated by deciduous species
	• Old growth and riparian areas
Mixed	• Areas where neither pine or deciduous species seemed to dominate
	• Often pine forests with young, dense deciduous growing in gaps
Scrub	• Short trees or shrubs (<6 meters tall)
	• Often very dense
High Grass	• Non-forested areas with relatively high (1 to 2 meters max height) non-woody plants
	• Recently cleared forested areas
	• Uncultivated fields
Low Grass	• Non-forested areas with relatively low (<1-meter max height) non-woody plants
	• Cultivated areas with short crops
	• Open fields/recently mowed

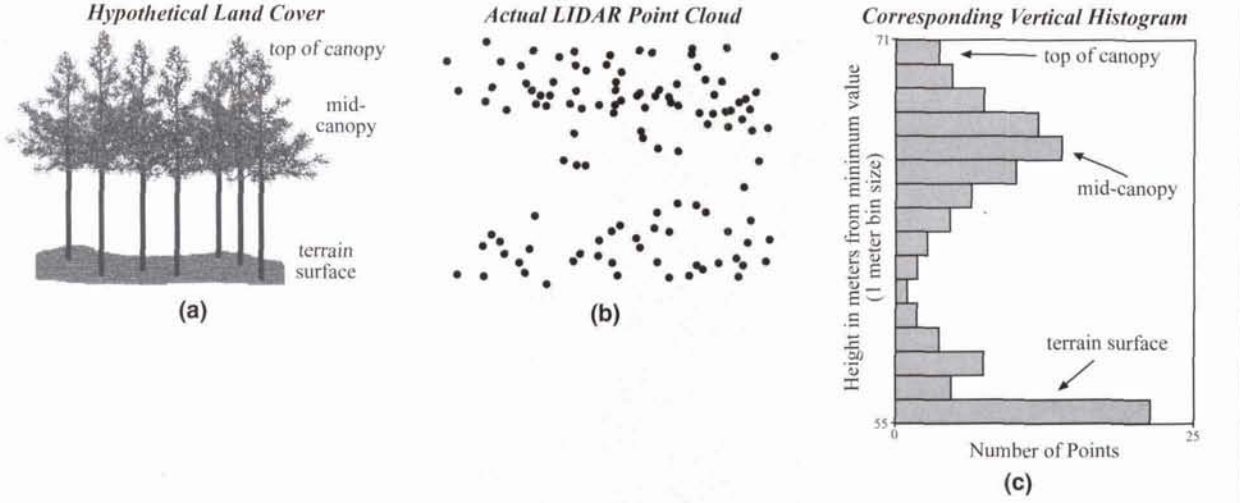

Figure 4. A terrestrial view of a hypothetical land cover scene (a), along with an actual lidar point cloud (b), and the corresponding vertical histogram of intercepted surfaces (c) that was created from the point cloud.

the center of the pixel represented by i and j; Z represents the set of the relative height values for the lidar points within a 15- by 15-m square surrounding the point represented by X_i and Y_j; and P is the mathematical notation for a percentile.

This technique yielded a ten-band statistical image. Of the possible ten bands, Plate 1a displays three in a color composite image. The red image plane contains the values of the relative Z-values of the point in which all of the other points in the kernel for that grid cell were below it (i.e., the maximum point). The green plane contains the relative Z-values of the point in which 40 percent of the points were below it. Finally, the blue plane contains the relative elevation value of the point in which 10 percent of the points were below it.

Shades of gray, including white and black, are present in areas where all the values were approximately equal to one another (i.e., all the points were near maximum points). Dense canopy prevented much lidar penetration, so nearly all of the points resided near the top of the distribution. This meant that the very bright-white areas represent the tallest canopy with the densest vegetation. An examination of the color-infrared imagery revealed that these areas usually contained bottomland-hardwood found in the riparian stream channels. The darker gray shades indicate shorter regions of very dense canopy. Finally, the very dark areas contain no trees. Like gray shades, blue hues represent areas where most of the points were near the maximum Z-value. These areas consist of shorter stands with even denser canopy. Yellowish-green hues represent areas with relatively high or balanced central region of the vertical histogram distribution. These areas consist of partially open canopy. Pure green areas contain shorter pine, particularly plantation pine, while red areas are indicative of open canopies typical of tall pine, or transitional areas between deciduous stands and open fields. Figure 5 depicts the curves associated with four land-cover types found at four specific pixel locations in the study area. *In effect, these curves represent a lidar-based signature for these land-cover classes.*

This ten-band image was classified using a supervised minimum-distance classification algorithm (Jensen, 1996). The classification was performed by selecting approximately 500 pixels for each class as training sites using the color-infrared aerial photography. These training sites were verified through *in situ* land-cover observation as previously discussed. The resulting classification map is shown in Plate 1b.

Assessment of Elevation Errors by Vegetation Class

The mean absolute vertical error was calculated for each of the lidar-derived vegetation classes using a DTM generated from the *automatic* dataset. An ANOVA was used to test for significant differences in this statistic. This test was conducted to validate the theory behind the creation of an adaptive vegetation removal algorithm. It was thought that if lidar-derived elevation error varied with vegetation type, it might be possible to minimize the error in a particular class. Reducing the error in any class would cause the overall elevation error to be reduced.

Mean absolute vertical error by land cover is shown in Table 2. The one-way ANOVA test revealed that there was a significant difference in the accuracy of the lidar-derived elevation information by lidar-derived land-cover class. Note that the errors in the open low- and high-grass areas are at or near the optimum error level and close to zero. The other vegetated areas could benefit from further algorithm refinement. For example, while the low-grass error may be near its optimum level, a more aggressive set of parameters for the lidar vegetation point removal algorithm could help minimize the elevation error in forested areas.

Algorithm Calibration (Optimization)

The process used to create the "automatic" lidar dataset is not without human intervention. It requires a human operator to determine the input parameters for the lidar vegetation point removal algorithm. The operator's decisions on what parameters to use are based on the theoretical error model discussed previously (Figure 1), and his or her own past experience. Using overly aggressive parameters can result in the semi-systematic interpolation error that is the result of shaving off small peaks and smoothing steep slopes. Parameters that are not as aggressive can result in over-prediction because non-ground points are left in the DTM. Often the operator decides to err in the latter direction, because during the manual editing process it is easier to see and remove unwanted points, than to detect the absence of valid points and reinstate them.

Creation of a truly comparable adaptive surface, in which the operator arbitrarily chooses algorithm parameters based on past experience, would be impossible, as well as undesirable. To overcome this problem, and create two comparable surfaces, it was decided to calibrate both the automatic and adaptive lidar

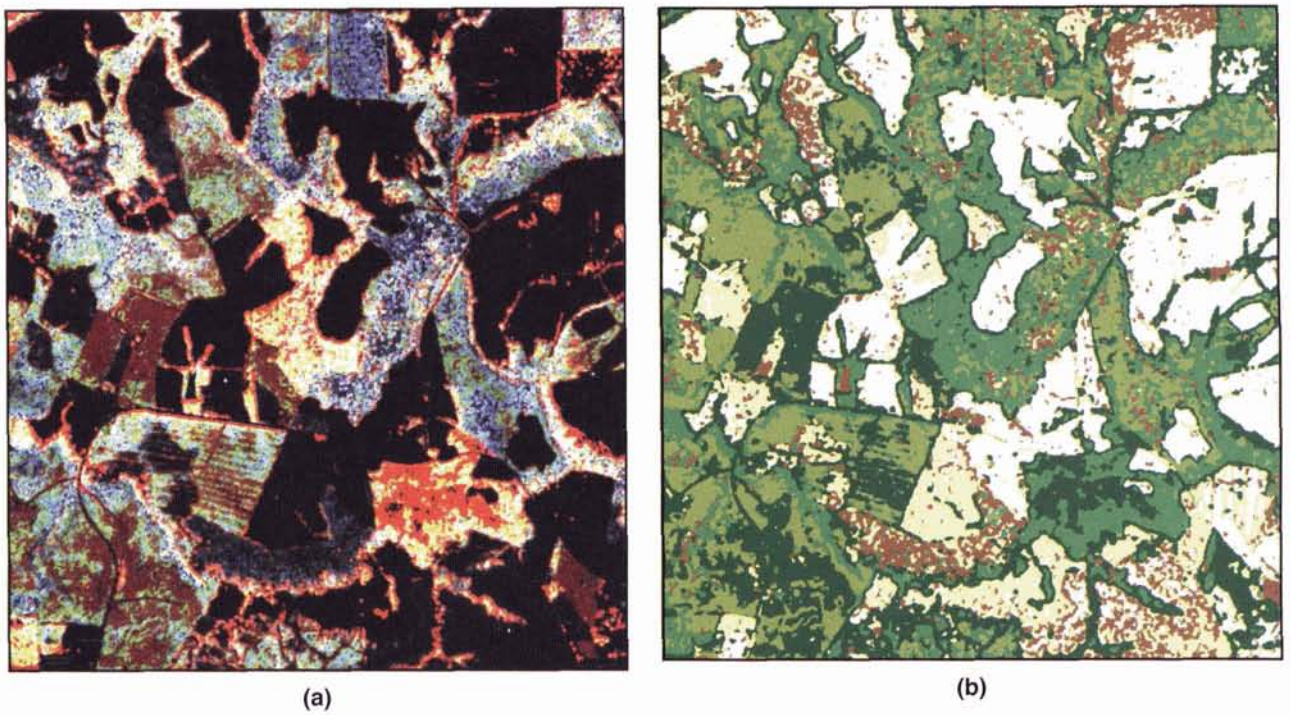

Plate 1. (a) A color composite created by displaying three of the ten bands of the lidar-derived statistical image described in the text. (b) A vegetation map produced by classifying the lidar-derived statistical image.

vegetation point removal techniques by using the reference elevation points, thus effectively optimizing these methods. This allowed both methods to be compared based on the best surface each could create. The optimization methodology systematically generated algorithm parameters, created a surface, and then tested the error for that surface (Figure 6). The process simultaneously derived (1) algorithm parameters for each land cover (based on the lidar-derived land-cover map), and (2) the entire set of elevation points. When this process was completed, two optimized surfaces existed. The *adaptive optimized automatic* surface was created by considering land cover in the optimization process. Conversely, the *optimized automatic* considered all the elevation points together (i.e., it ignored vegetation class).

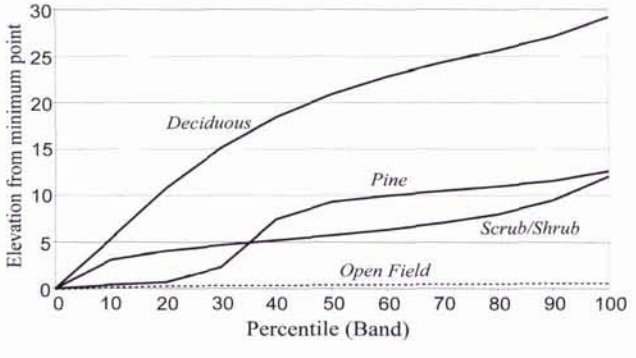

Figure 5. Lidar-derived signatures for selected pixels of known land cover contained in the statistical image shown in Plate 1a.

TABLE 2. THE MEAN ABSOLUTE ERRORS ASSOCIATED WITH EACH LIDAR-DERIVED VEGETATION CLASS IN THE DTM CREATED USING THE *AUTOMATIC* DATASET

Land Cover	# of Reference Points	Mean Absolute Vertical Error (m)
Low Grass	100	0.10
High Grass	73	0.27
Scrub	63	1.51
Pine	134	0.46
Deciduous	144	2.43
Mixed	134	2.42
Total	648	1.33

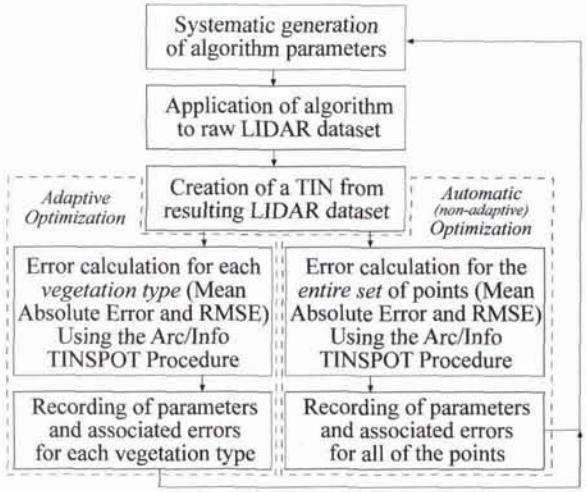

Figure 6. A flow diagram documenting the calibration process used to create optimized DTM surfaces for comparison. The process was implemented using a Visual Basic program that took advantage of Arc/Info's Open Development Environment (ODE) and a number of Arc Macro Language (AML) scripts.

Surface Form Accuracy of Various Lidar-Derived Digital Elevation Models

Surface form (slope and aspect) accuracy is often considered just as important as the vertical accuracy of DTMs. For example, when modeling the overland flow of liquids, it is vitally important to have a correct model of the shape or form of the surface. Because all the reference data were collected in transects, an overall assessment of surface form was not possible. However, it was possible to use the elevation information obtained along the transects. The slope was calculated between each *in situ* elevation point by converting the rise and run information between each point. This process was performed for each of the four lidar-derived test surfaces and compared with the slope derived from the *in situ* reference data. The absolute slope error was calculated by taking the absolute difference between the slope of the *in situ* reference information, and the slope of the surface derived using the lidar data. The mean of the absolute slope errors for each surface were then calculated and tested for significant differences from the adaptive surface using three *t*-tests.

Results

Lidar-Derived Vegetation Classification Map

The lidar-based vegetation classification map was smoothed using a 5- by 5-pixel majority filter to reduce noise. This was performed because the field surveys in which the reference data were collected did not account for isolated or small changes in land cover. The overall accuracy of the map was 72 percent with a Kappa Coefficient of Agreement of 0.65 (Table 3). One factor that may contribute to the confusion between classes is terrain variability. For example, if a steep elevation change occurs entirely within the kernel size (15 by 15 m), the signature from the vertical distribution of points may look more like a heavily vegetated area when in reality it is an open field or is void of vegetation entirely. A striking problem with this classification was the confusion between high grass and low grass. Basically, it was not possible to discriminate between low- and high-grass cover using the lidar data. However, when these classes were combined into a single "Open" class, the overall accuracy increased to 84 percent and the Kappa Coefficient of Agreement to 0.780. Based on these results, it was possible to reject hypothesis #1 and state that information contained in the vertical distribution of lidar points can be used to classify vegetation cover type.

TABLE 3. ACCURACY ASSESSMENT FOR THE LIDAR-DERIVED CLASSIFICATION. A LARGE AMOUNT OF CONFUSION EXISTS BETWEEN THE HIGH AND LOW CATEGORIES

	Reference Data							
	Low	High	Scrub	Pine	Mixed	Dec	Total	Users
Low	51	56					107	48%
High	7	70				1	78	90%
Scrub			14				14	100%
Pine	2	2	5	55	3	6	73	75%
Mixed			2	9	96	20	127	76%
Dec					36	94	130	72%
Total	60	128	21	64	135	121	529	
Producers	85%	55%	67%	86%	71%	78%		72%

Overall Accuracy = 72%—K-Hat = 0.65061
The overall accuracy was 84% and the K-Hat = 0.780 when high and low grass classes were combined.

Vertical Accuracy of DTMs Created Using Lidar Data

The differences in mean absolute vertical error and root-mean-squared error (RMSE) for the four DTMs created using the four alternative methods are displayed in Figure 7. Each of the *t*-tests were significant at the 0.01 level. Based on the significance of the *t*-tests, it was possible to reject hypothesis #2 and state that DTM vertical accuracy can be improved through an adaptive application of a lidar vegetation point removal algorithm that incorporates lidar-derived vegetation type information. The adaptive technique creates a superior DTM when compared to DTMs created in which vegetation is not accounted for in the application of the vegetation removal algorithm. As an additional note of clarification, the *automatic* dataset does not represent a commercial lidar product that would be delivered to a DTM user. Although the

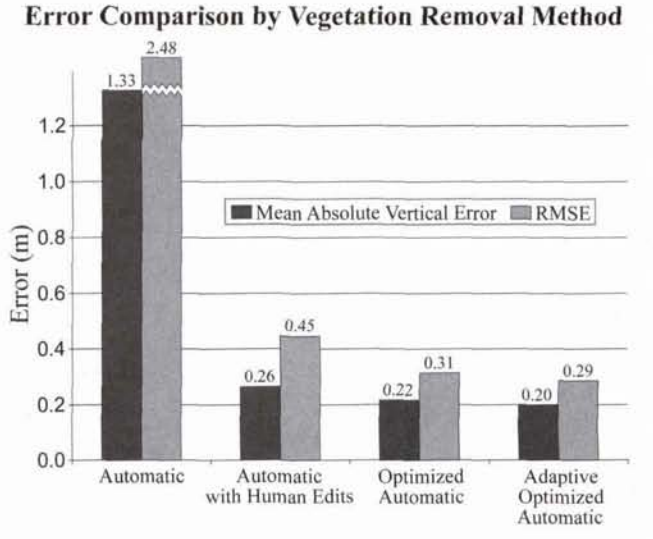

Figure 7. A comparison of the error found in each of the lidar-derived DTMs. The mean absolute error of the DTM produced using the adaptive optimized method was significantly smaller then all of the other techniques at the 0.01 level. These results indicate that an adaptive approach to vegetation point removal is of value.

automatic with human edits surface was processed identically to a consumer product, the lidar data for this project was acquired leaf-on. It has been shown that lidar-derived DTMs are less accurate when collected during leaf-on vs. leaf-off conditions (Raber *et al.*, 2002). This effect is a likely a contributor to the reason the DTM errors reported in Figure 7 are not consistent with commercial lidar accuracy claims.

Surface Form (Slope) Accuracy of Lidar-Derived DTMs

The slope error descriptive statistics associated with each method are summarized in Table 4. The DTM derived using the optimized adaptive method was significantly better then each of the DTMs created using alternative methods at the 0.05 level, except for the optimized automatic method which was not significantly different. Based on these results, it was possible to reject Hypothesis #3 and state that DTM surface form (slope) can be improved through an adaptive application of a lidar vegetation point removal algorithm that incorporates lidar-derived vegetation type information. However, the optimized automatic methodology and the optimized adaptive methodology produced surface form results that were for all practical purposes nearly identical.

Summary

Potential applications for vegetation classification based solely on lidar data are exciting. Refinement of the methodology discussed in this paper could result in the fully automated creation of a virtual reality visualization of an area that included elements of terrain and land cover based entirely on lidar data without the aid of aerial photography or other remote sensor data. Land-cover maps could be created at the same time lidar missions are flown, thus creating a new tool for land planners and foresters.

A DTM produced using an adaptive lidar vegetation point removal algorithm was more accurate than one produced using techniques that did not consider vegetation cover (Figure 7). The differences in DTM elevation error between the optimized adaptive and the optimized automatic algorithms (approximately 3 cm), as well as the differences between the optimized adaptive and the automatic with manual edits (approximately 13 cm), were not that large. However, these differences were statistically significant.

The method discussed in this paper classifies the lidar point distribution into land-cover classes and then uses elevation reference data to calibrate vegetation removal algorithm parameters for each land-cover class. Calibration requires minimal ground survey. However, there is potential for the development of a predictive relationship between the vertical distribution of lidar points and the algorithm parameters needed for a given area. Another topic for future research is the testing of this methodology using other lidar sensors, and under various physiographic and temporal conditions. It is important to note that the adaptive method requires no manual editing and little extra computer computation. Also, when humans edit lidar data to create and then refine a DTM, they (1) calibrate the algorithm parameters to their own past experiences, and (2) manually edit out points based on their own heuristic rules of thumb.

TABLE 4. SLOPE ERROR TABLE

DSM	Absolute Maximum Slope Error	Absolute Mean Slope Error	Significance (Different from Adaptive)
Automatic	53°	6.7°	0.0001
Automatic with Manual Edits	12°	1.6°	0.022
Optimized Automatic	12°	1.4°	0.994*
Optimized Adaptive	12°	1.4°	NA

*Not Significant

Conversely, when a DTM is produced using the adaptive algorithm applied to lidar data, it is possible to document explicitly the rules that were used to create the DTM.

Acknowledgments

The research presented in this paper was preformed at the NASA Affiliated Research Center at the University of South Carolina. This center is supported through a cooperative agreement with the NASA Commercial Remote Sensing Program at the John C. Stennis Space Center. The authors wish to thank Michael Hodgson, Jason Tullis, Laura Schmidt, Yingming Zhou, Chris Robinson, Karl Heidemann, and Neil Eggleston for their contributions to various aspects of the research.

References

Blair, J.B., and M.A. Hofton, 1999. Modeling laser altimeter return waveforms over complex vegetation using high resolution elevation data, *Geophysical Research Letters*, 26(16):2509–2512.

Cowen, D.J., J.R. Jensen, C. Hendrix, M.E. Hodgson, and S.R. Schill, 2000. A GIS-assisted rail construction econometric model that incorporates LIDAR data, *Photogrammetric Engineering & Remote Sensing*, 66(11):1323–1328.

Hodgson, M.E., J.R. Jensen, L. Schmidt, S.R. Schill, and B. Davis, 2003. An evaluation of LIDAR- and IFSAR-derived digital elevation models in leaf-on conditions with USGS Level 1 and Level 2 DEMs, *Remote Sensing of Environment*, in press.

Huising, E.J., and L.M.G. Pereira, 1998. Errors and accuracy of laser data acquired by various laser scanning systems for topographic applications, *ISPRS Journal of Photogrammetry and Remote Sensing*, 53:245–261.

Hyyppä, H., and J. Hyyppä, 1999. Comparing the accuracy of laser scanner with other optical remote sensing data sources for stand attribute retrieval, *The Photogrammetric Journal of Finland*, 16(2):5–15.

Hyyppä, J., and M. Inkinen, 1999. Detection and estimating attributes for single trees using laser scanner, *The Photogrammetric Journal of Finland*, 16(2):27–42.

Jensen, J.R., 1996. *Introductory Digital Image Processing A Remote Sensing Perspective*, Prentice-Hall, Inc., Upper Saddle River, New Jersey, 318 p.

———, 2000. *Remote Sensing of the Environment: An Earth Resource Perspective*, Prentice-Hall, Inc., Upper Saddle River, New Jersey, 544 p.

Jensen, J.R., M.E. Hodgson, H.E. Mackey, and W. Krabill, 1987. Correlation between aircraft and LIDAR remotely sensed data on a forested wetland, *Geocarto International*, 4:39–54.

Kraus, K., and N. Pfeifer, 1998. Determination of terrain models in wooded areas with airborne laser scanner data, *ISPRS Journal of Photogrammetry and Remote Sensing*, 53:193–203.

Lefsky, M.A., W.B. Cohen, S.A. Acker, G.G. Parker, T.A. Spies, and D. Harding, 1999. LIDAR remote sensing of the canopy structure and biophysical properties of Douglas-fir western hemlock forests, *Remote Sensing of Environment*, 70:339–361.

Maune, D.F. (editor), 2001. *Digital Elevation Model Technologies and Applications: The DEM Users Manual*. The American Society for Photogrammetry and Remote Sensing, Bethesda, Maryland, 539 p.

Means, J.E., S.A. Acker, D.J. Harding, J.B. Blair, M.A. Lefsky, W.B. Cohen, M.E. Harmon, and W.A. McKee, 1999. Use of large footprint LIDAR to estimate forest stand characteristics in the western Cascades of Oregon, *Remote Sensing of Environment*, 67:298–308.

Means, J.E., S.A. Acker, B.J. Fitt, M. Renslow, L. Emerson, and C.J. Hendrix, 2000. Predicting forest stand characteristics with airborne scanning LIDAR, *Photogrammetric Engineering & Remote Sensing*, 66(11):1367–1371.

Næsset, E., 1996. Determination of mean tree height of forest stands using airborne laser scanner data, *ISPRS Journal of Photogrammetry and Remote Sensing*, 60(3):327–334

Plaut, J.J., B. Rivard, and M.A. D'Iorio, 1999. Radar: Sensors and case studies, *Remote Sensing for the Earth Sciences: Manual of Remote*

Sensing, Third Edition, Volume 3 (A.N. Rencz, editor), John Wiley and Sons, New York, N.Y., pp. 613–642.

Raber, G.T., M.E. Hodgson, J.R. Jensen, J.A. Tullis, G. Thompson, B. Davis, and K. Schuckman, 2002. Comparison of LIDAR data collected leaf-on vs. leaf-off for the creation of digital elevation models, *Proceedings of the ASPRS 2002 Annual Convention*, 19–26 April, Washington, D.C. (American Society for Photogrammetry and Remote Sensing, Bethesda, Maryland), unpaginated CD-ROM.

(Received 03 October 2001; accepted 12 March 2002; revised 19 April 2002)